Comprehensive Genetic Analysis Unraveled the Missing Heritability in a Chinese Cohort With Wolfram Syndrome 1: Clinical and Genetic Findings

Xin Zhang, Yue Xie, Ke Xu, Haoyu Chang, Xiaohui Zhang, and Yang Li

Beijing Institute of Ophthalmology, Beijing Tongren Eye Center, Beijing Tongren Hospital, Capital Medical University, Beijing Ophthalmology & Visual Sciences Key Lab. Beijing, China

Correspondence: Yang Li, Beijing Institute of Ophthalmology, Beijing Tongren Hospital, Hougou Lane 17, Chong Nei Street, Beijing 100730, China;
yilbio@163.com.

Xin Zhang and Yue Xie contributed equally.

Received: May 12, 2022
Accepted: August 18, 2022
Published: September 13, 2022

Citation: Zhang X, Xie Y, Xu K, Chang H, Zhang X, Li Y. Comprehensive genetic analysis unraveled the missing heritability in a Chinese cohort with wolfram syndrome 1: Clinical and genetic findings. *Invest Ophthalmol Vis Sci.* 2022;63(10):9.
https://doi.org/10.1167/iovs.63.10.9

Purpose. To identify the missing heritability of patients with Wolfram syndrome 1 (WFS1) in a Chinese cohort and to report their clinical and genetic features.

Methods. We recruited 24 unrelated patients with suspected WFS1 who carried at least one variant in *WFS1*. All patients underwent ophthalmic examinations and comprehensive molecular genetic analyses, including Sanger-DNA sequencing of *WFS1* and next-generation sequencing of the whole *WFS1* sequence.

Results. We identified 38 distinct pathogenic variants of *WFS1* in the 24 probands, comprising 23 patients with biallelic variants and one patient with a monoallelic variant. Sanger-DNA sequencing of *WFS1* initially detected 35 variants, and subsequent whole genome sequencing revealed three missing variants: one novel deep intronic variant (DIV), one copy number variant (CNV), and one variant in the promoter region. Minigene assays showed that the DIV activated cryptic splice sites, leading to the insertion of pseudoexons. Optic atrophy was observed in all patients, and diabetes mellitus (DM) was revealed in 21 patients (91.3%), hearing loss in nine patients (39.1%), renal tract abnormalities in nine patients (39.1%), and diabetes insipidus in five patients (21.7%). The mean onset age for DM was significantly younger in the patients with biallelic null variants than in the patients with biallelic missense variants.

Conclusions. Our results extend the pathogenic variant spectrum of *WFS1*. DIVs and CNVs explained rare unresolved Chinese cases with WFS1. The patients showed a wide and variable clinical spectrum, supporting the importance of genetic analysis for patients with atypical WFS1.

Keywords: *WFS1*, deep intronic variant, copy number variation

Wolfram syndrome 1 (WFS1, OMIM 222300) is a rare autosomal recessive disorder with a prevalence between 1/770,000 and 1/54,478.[1–6] The major clinical manifestations comprise diabetes insipidus (DI), diabetes mellitus (DM), optic atrophy (OA), and deafness (D); consequently, the syndrome is sometimes referred to as DIDMOAD. Other clinical features include urological and neurological defects.[1,4–6] Urinary tract dysfunction (UD) occurs more frequently than previously assumed, so WFS1 is also sometimes denoted by the acronym DIDMOADUD.[2] The nature history of this progressive neurodegenerative disorder indicates that most patients develop neurologic abnormalities, including cerebellar ataxia, peripheral neuropathy, dementia, and psychiatric illness.[5] Most patients have shortened lifespans, with an average age of 30 years (range 25–49), as a consequence of central respiratory failure from brain stem atrophy.[2,7] Currently, no therapeutic intervention is available to alter the progression or improve the life expectancy of affected individuals.[7]

WFS1 is caused by pathogenic variants of the *WFS1* gene (NM_006005), which is located on chromosome 4p16.1.[8,9] The gene, composed of eight exons, encodes wolframin, an 890-amino-acid transmembrane glycoprotein located in the endoplasmic reticulum.[9,10] Wolframin was hypothesized to have an involvement in membrane trafficking, protein processing, or regulation of endoplasmic reticulum calcium homeostasis.[9,10] *WFS1* is ubiquitously expressed, but its expression levels differ significantly among organs, with the highest transcript levels reported in the mouse brain, pancreas, and heart, followed by the liver and low expression in the kidney and spleen.[9,10] At present, 496 *WFS1* variants have been reported based on the Human Gene Variant Database Professional 2021.4; most of these variations occur in exon 8. The majority of the reported pathogenic variants of the *WFS1* gene are missense variants and small deletion/insertion (<20bp) variants, followed by nonsense variants,[2,5,11] whereas splicing variants and gene rearrangements are rarely identified.[12–14]

Heterozygous pathogenic variants of *WFS1* can lead to a group of autosomal dominant genetic diseases called *WFS1*-related disorders, which include Wolfram-like syndrome (WFSL, OMIM 614296) and DFNA6/14/38 (OMIM 600965).[7,15] In contrast to typical WFS1, the critical features of patients with WFSL are progressive optic

atrophy and sensorineural hearing loss with/without impaired glucose regulation,[7,15,16] whereas the essential characteristic of patients with DFNA6/14/38, known as autosomal dominant non-syndromic hearing loss, is a form of low-frequency sensorineural hearing loss.[15,16]

In the present study, we conducted a comprehensive molecular analysis of 24 unrelated patients with suspected WFS1 carrying at least one pathogenic variant of *WFS1*. We reported 18 novel variants, including three missing alleles, revealed by whole genome sequencing (WGS). Minigene analysis confirmed one novel deep intronic variant that resulted in the insertions of two pseudoexons (PEs). We also documented the clinical features of the patients and their genotype-phenotype relationships.

Methods

Patients

All research procedures of this study were conducted according to the instructions of the Beijing Tongren Hospital Joint Committee on Clinical Investigation and the principles of the Declaration of Helsinki. In total, 24 unrelated patients (17 males and 7 females) were recruited from 2099 probands diagnosed with suspected hereditary optic neuropathy (HON), who were from the Genetics Laboratory of Beijing Institute of Ophthalmology, Beijing Tongren Eye Center. Among the 2099 patients, almost 70% of them carried primary disease-causing variants in mtDNA associated with Leber's HON, 13% of them had variants in *OPA1*, and the remaining patients either harbored variants in another less frequent HON genes or without knowledge of genotype. All the enrolled patients were clinically diagnosed with suspected WFS1, carried at least one pathogenic or likely pathogenic variant of the *WFS1* gene, and not harbored any disease-causing variants in mtDNA associated with LHON and *OPA1*. The criterion for a suspicion of WFS1 was that the patients had at least two clinical features of WFS1.[2] Among the 24 probands who all were of Chinese Han ethnicity, three patients were from consanguineous marriages, three had one sibling with similar symptoms, and the remaining 18 were sporadic cases. After collecting the medical records and examination results from the endocrinology, otolaryngology, urology, and other related departments, all patients underwent detailed ophthalmic examinations, including best-corrected visual acuity (BCVA), slit-lamp biomicroscopy, and fundus examination. A total of 19 patients underwent optical coherence tomography (OCT) and color vision evaluation by the Lanthony Panel Hue15 or Farnsworth Panel D15, and half of the patients underwent visual field and visual evoked potential examinations. We also followed up on six patients by telephone surveys.

PCR-Based Sequencing of the *WFS1* Gene

After informed consent was obtained, peripheral blood samples were collected from all patients and from their available relatives for genetic assessment. Genomic DNA was extracted using genomic DNA extraction and purification kits (Vigorous, Beijing, China) following the manufacturer's protocol. Whole exons and exon-intron boundaries of the *WFS1* gene were amplified by PCR using the primers listed in Supplementary Table S1. The purified PCR amplicons were directly sequenced on an ABI Prism 373A DNA sequencer (Applied Biosystems, Foster City, CA, USA). The sequencing results were compared to the published cDNA sequence of *WFS1* (GenBank NM_006005). Co-segregation analysis was performed whenever the DNA of any family members was available.

Identification of a Large Deletion

We inferred the existence of a large deletion of *WFS1* in patient A3784, as no exons could be amplified by PCR. We performed gap PCR and long-range PCR assays to determine the location of the breakpoint junctions using several pairs of primers (Supplementary Table S1).

WGS and Variant Bioinformatics Analysis

We performed WGS to detect the missing variants in four patients (A2018, A3537, A3742, and A4170) who had only one pathogenic variant detected using MGI, as previously described.[17,18] In brief, the WGS libraries were sequenced on the DNBSEQ-T7 platform (MGI Tech) using a 100 bp paired-end mode with a 30-fold minimal median coverage per genome. The data were mapped to the human genome GRCh37/hg19 with the Burrows–Wheeler Aligner. Variant calling was performed by GATK v4.1.4.1 and variants were annotated using ANNOVAR software. A comparison was also conducted using the genome aggregation database (gnomAD, https://gnomad.broadinstitute.org/, accessed March 14, 2021) to exclude nonpathogenic polymorphisms. Five algorithms, including Human Splicing Finder (version 2.4.1), Alternative Splice Site Predictor (version 2011-10-01), MaxEntScan (version 2003-7-22), NetGene2 (version 2.42), and NNSplice (version 0.9) were used to assess the possibility that noncoding region variants would induce aberrant transcript splicing.

Variants were selected for further testing by in vitro minigene assays when they were located at putative splice sites with a relative strength of at least 60% of the maximal score in at least two of five splice prediction programs or when they led to an increased splice prediction score of at least 30% compared to the WT. NetUTR server (https://services.healthtech.dtu.dk/service.php?NetUTR-1.0) was used to predict the effect of the variant on 5′UTR splice sites. The CNVs were analyzed preliminarily from variations in the read depth using CNV kit software. Sequencing reads using Integrative Genomics Viewer (IGV) software were examined to locate the breakpoints, and Sanger sequencing was performed across the predicted breakpoints to confirm the breakpoint junctions. The sequences of all primers are listed in Supplementary Table S1.

Minigene Assay in HEK293T Cells

A novel deep intron variant (DIV) c.712+681C>T was highly suspected to cause splicing abnormalities; therefore this DIV was evaluated for an effect on splicing with the pET01-based exon trapping system (Exontrap, MoBiTec GmbH, Goettingen, Germany). The cloned 4078bp fragment, including the DIV c.712+681C>T and exons 6 and 7 (upstream and downstream), was PCR amplified from the genomic DNA of patient A4170 using the primers listed in Supplementary Table S1. The authentication of HEK293T cells was verified by short tandem repeat analysis (Supplementary Table S2). The cells were transfected with 2.5 µg of the selected minigene plasmids using Lipofectamine

Investigative Ophthalmology & Visual Science

2000 DNA transfection reagent (Invitrogen, Carlsbad, CA, USA). After 48 hours, the transfected cells were harvested, and total RNA was extracted using an EndoFree Plasmid Maxi Kit (Qiagen, Hilden, Germany). Reverse transcription PCR (RT-PCR) was performed with a pair of specific primers (ETPR04 and ETPR05 in the exons V1 and V2 of pET01) and the FastKing One-Step RT-PCR Kit (Tiangen Biotech, Beijing, China). The products were separated by electrophoresis on 2% agarose gels, excised, and sequenced.

Statistical Analysis

We converted the Snellen ratios into the logarithm of the minimum angle of resolution (logMAR) values for statistical purposes. The logMAR values of 0, 1.0, 1.85, 2.3, and 2.7 are equal to a Snellen vision of 1.0, 0.1, counting fingers, hand movements, and light perception, respectively. The Shapiro-Wilk test was used to evaluate whether a single group of data had a normal distribution. The Kruskal-Wallis test was used to evaluate any difference between two groups with data that were not normally distributed. The Pearson correlation coefficient and linear regression analysis were used to evaluate the association of BCVA in both eyes. A P value <0.05 was considered statistically significant.

Results

WFS1 Gene Variants

We identified a total of 38 distinct *WFS1* variants in the 24 probands, who included 23 patients with identified biallelic variants and one patient with only one variant detected. Sanger DNA sequencing and the gap PCR of *WFS1* initially detected 35 variants, which comprised 20 missense variants, nine small insertion/deletions (7 frameshift, 2 non-frameshift), five nonsense variants, and one large deletion. Subsequent WGS revealed three novel missing variants, which comprised one DIV, one large duplication, and one variant in the 5′ untranslated region (5′UTR) (Table 1). The novel variant (c.−6+6T>C) in the 5′UTR was predicted by the NetUTR server to eliminate the first donor splicing site (Supplementary Table S3). Among the 38 variants, 18 were first identified in the current study. All the novel variants were either not recorded in any public database or were present at a very low frequency, and all were defined as pathogenic or likely pathogenic based on the ACMG guidelines and standards (Table 1). Almost 90% of the variants occurred in exon 8, whereas the remaining four variants were scattered in exons 4 and 5, intron 6, and intron 1 (5′ UTR). Two common variants were p. (Gly674Arg) and p. (Ala370Argfs*76); each was detected four and three times.

Table 1. Presumed Pathogenic *WFS1* Variants Identified in This Study and Analysis of the Variants by Predictive Programs

	Nucleotide Change NM_006005	Protein Effect	Variant Type	Allele Numbers	Polyphen2 HumDiv	Polyphen2 HumVar	Mutation Taster	SIFT	1000G ALL/EAS	gnomeAD ALL/EAS	Source	ACMG
Intron 1	c.-6+6T>C	p.(?)	SP	1	—	—	—	—	—	—	Novel	LP*
Exon 4	c.453_460+6delins20bp‡	p.(Asp151Glufs*3)	FS	1	—	—	DC	—	—	—	Novel	P
Exon 5	c.505G>A	p.(Glu169Lys)	MS	1	PD	PD	DC	T	—	0.00002/0.00005	2	P
Intron 6	c.712+681C>T	p.Gly238Lysfs*27	DI	1	—	—	—	—	—	—	Novel	LP†
Exon 8	c.1037C>T	p.(Pro346Leu)	MS	1	PD	PD	DC	D	—	0.00002/0.0001	28	P
Exon 8	c.1097_1107dup	p.(Ala370Argfs*76)	FS	3	—	—	DC	—	—	—	29	P
Exon 8	c.1174C>T	p.(Gln392*)	NS	1	—	—	DC	—	—	—	30	P
Exon 8	c.1235T>C	p.(Val412Ala)	MS	1	PD	PD	DC	D	0.001/0.007	0.001/0.009	15	P
Exon 8	c.1283C>A	p.(Pro428His)	MS	1	PD	PD	DC	D	—	—	Novel	LP
Exon 8	c.1285T>C	p.(Cys429Arg)	MS	1	PD	PD	DC	T	—	0.000008/0.0001	Novel	LP
Exon 8	c.1300_1302del	p.(Val434del)	IF	1	—	—	P*	—	—	—	31	P
Exon 8	c.1403dup	p.(Ser469Ilefs*74)	FS	1	—	—	DC	—	—	—	Novel	P
Exon 8	c.1424C>T	p.(Pro475Leu)	MS	1	PD	B	DC	T	-	0.000016/0	Novel	LP
Exon 8	c.1523_1524del	p.(Tyr508Cysfs*34)	FS	1	—	—	DC	—	—	—	32	P
Exon 8	c.1525_1539del	p.(Val509_Tyr513del)	IF	1	—	—	P*	—	—	—	6	P
Exon 8	c.1553T>C	p.(Met518Thr)	MS	1	PD	PD	DC	D	—	—	Novel	LP
Exon 8	c.1600T>G	p.(Tyr534Asp)	MS	2	PD	PD	DC	T	—	—	Novel	LP
Exon 8	c.1618T>G	p.(Trp540Gly)	MS	1	PD	PD	DC	D	—	—	Novel	LP
Exon 8	C.1672C>T	p.(Arg558Cys)	MS	1	PD	PD	DC	D	—	0.001/0	13	P
Exon 8	c.1673G>A	p.(Arg558His)	MS	1	PD	PD	DC	D	—	0.000068/0.000109	2	P
Exon 8	c.1885C>T	p.(Arg629Trp)	MS	1	PD	PD	P*	T	0.0002/0	0.00001/0	2	P
Exon 8	c.1956C>G	p.(Tyr652*)	NS	1	—	—	DC	—	—	—	Novel	LP
Exon 8	c.1997G>A	p.(Trp666*)	NS	1	—	—	DC	—	—	—	31	P
Exon 8	c.2006A>G	p.(Tyr669Cys)	MS	1	PD	PD	DC	D	—	—	32	P
Exon 8	c.2020G>A	p.(Gly674Arg)	MS	4	PD	PD	DC	D	0.0002	0.0002/0.0002	2	P
Exon 8	c.2070_2079del	p.(Cys690Trpfs*17)	FS	1	—	—	DC	—	—	—	Novel	P
Exon 8	c.2100G>T	p.(Trp700Cys)	MS	1	PD	PD	DC	D	–	–	12	P
Exon 8	c.2146G>A	p.(Ala716Thr)	MS	1	PD	PD	DC	T	—	0.000004/0	15	P
Exon 8	c.2168T>C	p.(Leu723Pro)	MS	2	PD	PD	DC	D	—	—	13	P
Exon 8	c.2171C>G	p.(Pro724Arg)	MS	1	PD	PD	DC	D	—	—	Novel	LP
Exon 8	c.2217C>A	p.(Tyr739*)	NS	1	—	—	DC	—	—	—	Novel	P
Exon 8	c.2425G>T	p.(Glu809*)	NS	2	—	—	DC	—	—	—	33	P
Exon 8	c.2534T>G	p.(Ile845Ser)	MS	1	PD	PD	DC	T	—	0.00002/0.00027	Novel	LP
Exon 8	c.2576G>C	p.(Arg859Pro)	MS	1	PD	PD	DC	D	—	—	15	P
Exon 8	c.2643_2646del	p.(Phe882Serfs*69)	FS	1	—	—	DC	—	—	—	34	P
Exon 8	c.2643_2644del	p.(Phe883Leufs*56)	FS	1	—	—	DC	—	—	—	Novel	P
Exon 8	c.928_1183dup	p.(Val395Glyfs*232)	CNV	1	—	—	—	—	—	—	Novel	P
Exon 8	g.6237437-6307683del	p.(?)	CNV	2	–	–	–	–	–	–	Novel	P

B, benign; CNV, copy number variant; D, damaging; DC, disease causing; EAS, east Asian; FS, frameshift; IF, in-frame; LP, likely pathogenicity; MS, missense; NS, nonsense; SP, splicing; P, pathogenicity; P*, polymorphism; PD, probably or possibly damaging; T, tolerated.

* NetUTR predicted to induce aberrant splicing.

† Five algorithms (Human Splicing Finder, Alternative Splice Site Predictor, MaxEntScan, NetGene2, and NNSplice) predicted to induce aberrant splicing.

‡ Full sequence: GGCTTAGAACAGCCTCTAAG.

Investigative Ophthalmology & Visual Science

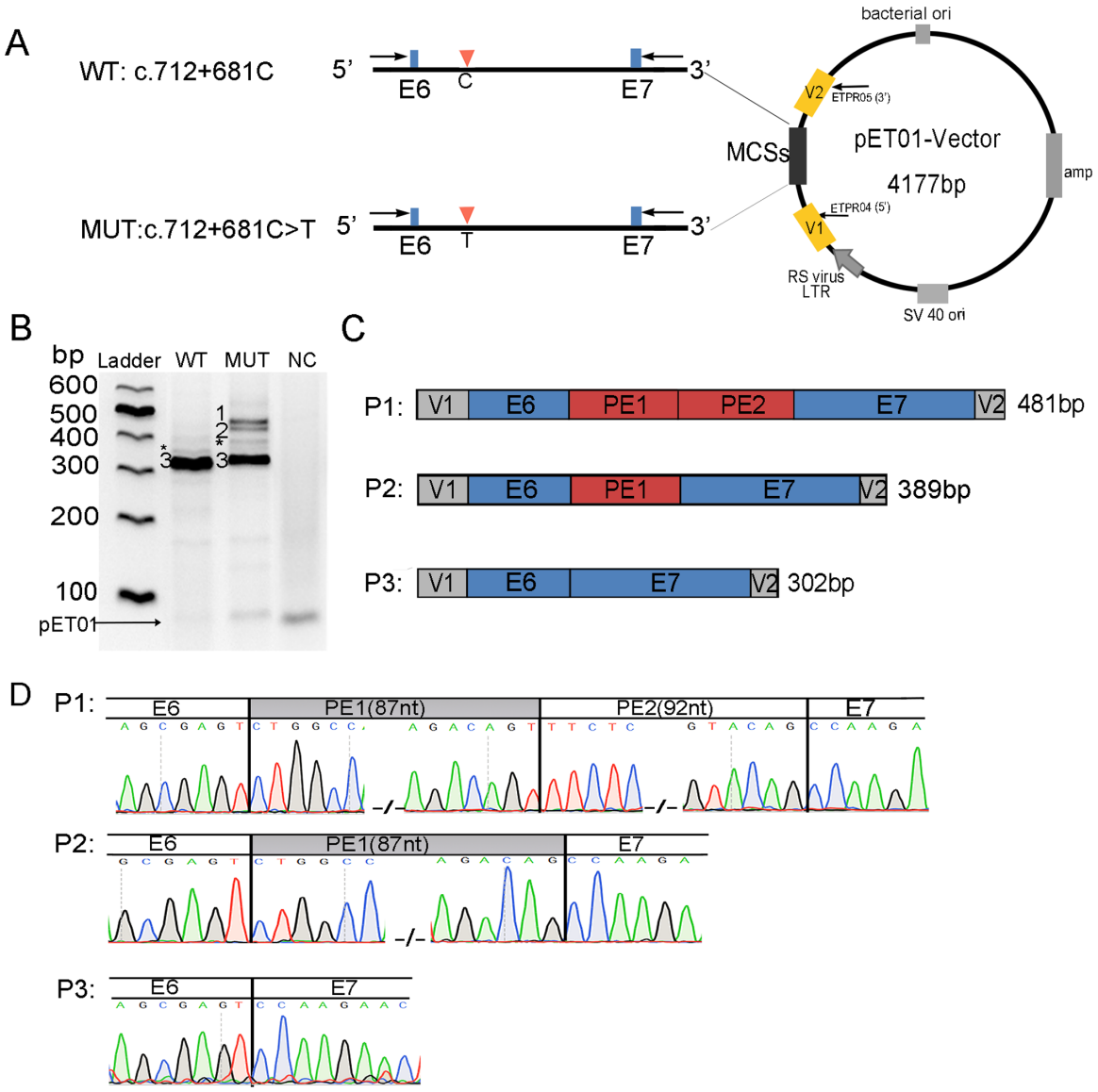

Figure 1. Outline of splice defects due to one deep intronic variant c.712+681C>T of the *WFS1* gene in minigene assays. The wild-type (WT) and mutant-type (MUT) minigenes were transfected into HEK293T cells, and their RNAs were subjected to RT-PCR. The cDNA was amplified using primers ETPR04 and ETPR05 in the exons of pET01. (**A**) Schematic representations of the WT and MUT constructors. Blue rectangles indicate exons and red triangles indicate the location of the splice variant sites. (**B**) RT-PCR and gel analysis for the WT, MUT, and empty vector (NC) minigenes show different splicing results. Two defects (fragments P1 and P2) were observed next to the WT fragments (fragment P3) in the MUT. Asterisks denote fragments for which no sequence information was obtained. (**C**) Schematic representation revealing details of the three splicing fragments. (**D**) Sanger-DNA sequencing of the two defects and one WT fragments. E, exon; V, vector exon; P, product.

The remaining 36 variants were detected either once (32/38, 84.2%) or twice (4/38, 10.5%).

A Novel DIV Validated by Minigene Assays

We identified one novel heterozygous DIV c.712+681C>T in patient A4170. The scores for the splice predictors for the DIV met the inclusion criteria of the minigene assay (Supplementary Table S2). Bioinformatic analyses suggested that the DIV triggered cryptic splice donor sites and resulted in the insertion of PEs (Supplementary Table S4). RT-PCR analysis revealed that the DIV caused two abnormal splicing products (P1 and P2) and one correctly spliced product P3 (Fig. 1). The product P1 included an 87-nt PE1 and a 92-nt PE2, whereas the product P2 only contained the PE1 (Fig. 1). Both the product P1 and P2 were predicted to produce a premature termination codon (PTC) p.(Val395Glyfs*232) (Supplementary Table S4).

CNV Analysis

Gap-PCR revealed a homozygous 70247 base pair (70 kb) deletion encompassing the entire *WFS1* genome in patient A3784, and WGS revealed a heterozygous c.928_1183dup (256 bp duplication) in patient A2018. The breakpoints of these two novel CNVs were both validated by Sanger DNA sequencing (Fig. 2). Bioinformatics analyses showed microhomology at the breakpoints and the potential

Investigative Ophthalmology & Visual Science

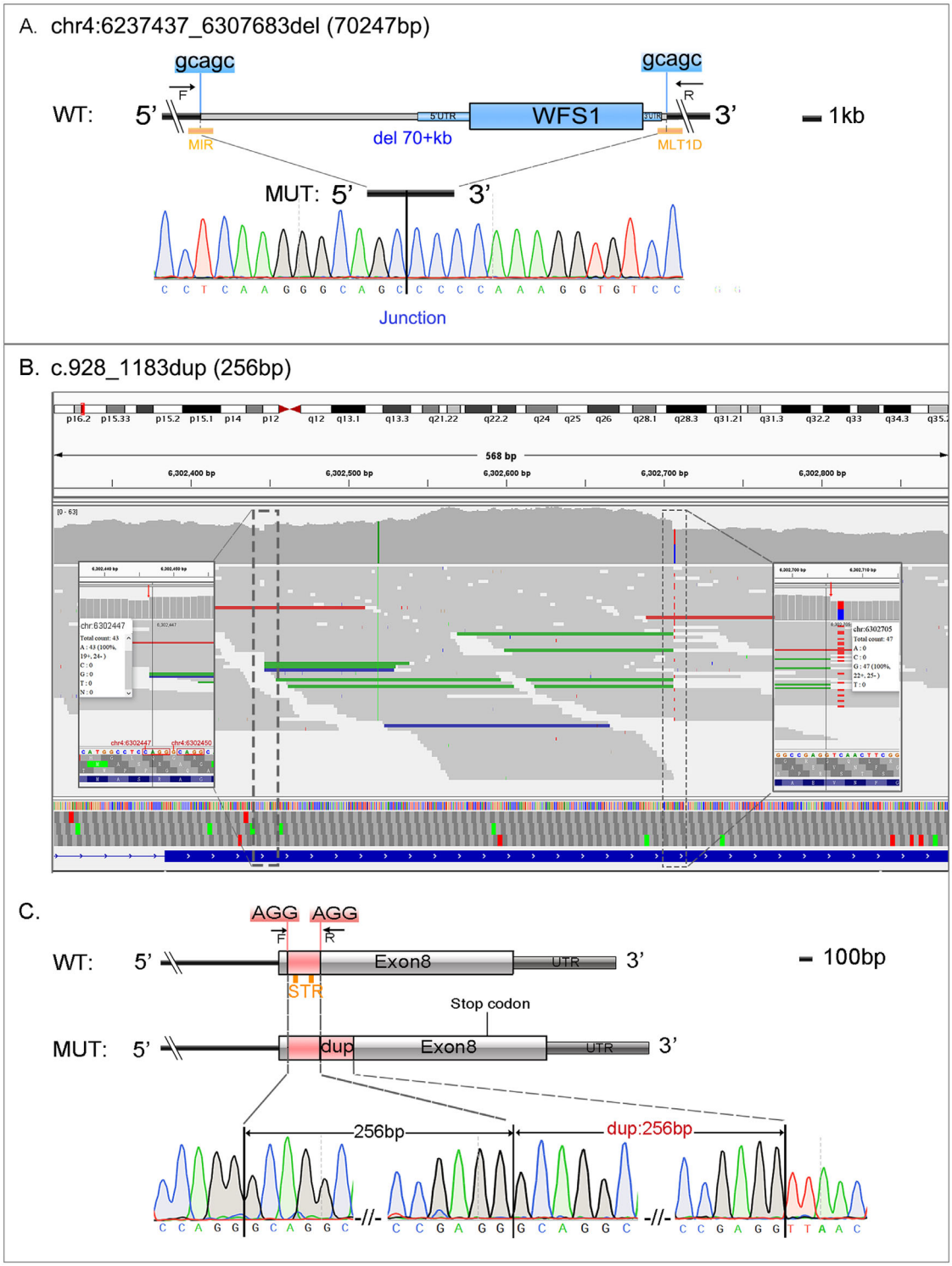

Figure 2. A gross deletion (chr4:6237437_6307683del) and one large duplication (c.928_1183dup) of the *WFS1* were identified in the current study. The primers used in PCR are depicted as *black arrows*. The *WFS1* sequences involved in the deletions and duplications are visualized as *blue* and *red rectangles*, respectively. (**A**) A schematic representation showing a homozygous 70kb gross deletion identified in patient 3784 and the breakpoint region (*black line*) revealed by Sanger sequencing. The "*gcagc*" on the top *blue rectangles* represents microhomology domains; MIR and MLT1D repetitive elements, represented by *orange rectangles*, are identified at the breaking boundaries. (**B**) The IGV plot showed a large heterozygous duplication in exon 8 in patient A2018. The region and the breakpoint were identified because of a sharp increase in the coverage and the increase in truncated reads. (**C**) Schematic representations show the 256bp tandem duplication in exon 8. Sanger-DNA sequencing revealed the proximal, junction, and distal breakpoints. The "*AGG*" on the top *pink rectangles* represents microhomology domains; two STR motifs, represented by orange rectangles, show non-B DNA motifs identified at both boundaries. STR, short tandem repeat.

Investigative Ophthalmology & Visual Science

Table 2. Clinical Features and Results of the *WFS1* Gene Variants Screening of the Patients

			BCVA (OD/OS)		Onset Age (Year)					Color Blindness	Other	*WFS1* Variants	
Patient ID	Gender	Exam Age	Snellen	logMar	DM	OA	DI	D	UD	(OD/OS)	Manifestations	Allele1	Allele2
A534	F	36	0.1/0.1	1.0/1.0	32	33	—	—	—	NA	—	p.(G674R)	p.(G674R)
A600	F	43	0.1/0.06	1.0/1.22	21	25	41	—	41	NA	Cataract, od	p.(R558C)	p.(P724R)
A610	M	31	0.02/FC	1.7/1.85	21	8	—	—	29	NA	—	p.(R629W)	p.(I845S)
A788	M	16	0.03/0.05	1.52/1.3	3	11	—	—	—	NA	Od	p.(A370Rfs*76)	p.(W700C)
A792	M	7	0.2/0.5	0.7/0.3	4	4	—	#9	—	G/G	Cataract, TOF, BI	p.(A370Rfs*76)	p.(A370Rfs*76)
A860	M	7	0.3/0.2	0.52/0.7	5	6	—	—	7	NA	OS:RAPD(+), cataract, BI	p.(P428H)	p.(S469Ifs*74)
A1041	M	19	0.07/0.1	1.15/1.0	5	14	—	—	—	T/T	OD:RAPD(+)	p.(E169K)	p.(G674R)
A1972	M	10	0.4/0.6	0.4/0.22	3	9	10	10	—	T/G	—	p.(D151Efs*3)	p.(V434del)
A2018	M	16	0.5/0.5	0.3/0.3	4	13	—	5	16	G/G	Cataract	p.(V509_Y513del)	c.928_1183dup
A2072	M	9	0.1/0.08	1.0/1.1	8	8	—	—	8	G/G	Cataract	p.(W540G)	p.(F883Lfs*56)
A2363	F	7	0.2/0.15	0.7/0.82	5	7	—	#9	–	YB/T	—	p.(Y534D)	p.(Y534D)
A2764	M	36	0.1/0.02	1.0/1.7	–	28	—	—	34	T/T	—	p.(C429R)	p.(C690Wfs*17)
A3301	M	17	0.08/0.04	1.1/1.4	10	12	—	—	17	G/G	Nystagmus, cataract	p.(L723P)	p.(L723P)
A3537	M	11	0.8/0.6	0.1/0.22	9	8	—	10	—	R/RG	#died around 13 y	p.(P346L)	c.-6+6T>C
A3784	F	12	0.25/0.15	0.6/0.82	3	9	—	9	—	T/RG	#MD (14y)	g.6237437-6307683del	g.6237437-6307683del
A3790	M	13	0.1/0.3	1.0/0.52	2	7	13	13	—	RG/RG	—	p.(Y669C)	p.(F881fs*69)
A3840	M	14	0.3/0.2	0.52/0.7	13	13	14	—	—	T/T	#depression & FI (16y)	p.(Y508Cfs*34)	p.(A716T)
A3989	F	10	0.2/0.2	0.7/0.7	2	9	—	10	10	RG/RG	—	p.(E809*)	p.(E809*)
A4048	F	11	0.7/0.7	0.16/0.16	9	9	—	—	—	NA	—	p.(V412A)	p.(Y652*)
A4170	F	29	0.02/0.02	1.7/1.7	12	18	—	—	—	RG/RG	—	p.(M518T)	c.712+681C>T
A4212	M	20	0.4/0.4	0.4/0.4	19	15	—	—	—	RG/RG	—	p.(R558H)	p.Y739*
A4581	M	16	0.6/0.6	0.22/0.22	12	14	–	15	—	T/T	—	p.(Q392*)	p.(G674R)
A4831	M	6	0.4/0.5	0.4/0.3	—	5	5	—	6	G/B	BI, #BPD (7y)	p.(P475L)	p.(W666*)
A3742	M	28	1.0/0.4	0/0.4	—	21	—	21(LF)	—	G/RG	OS: RAPD(+)	p.(R859P)	—

B, blue; BI, balance impairment; BPD, bipolar disorder; D, deafness; F, female; FI, fecal incontinence G, green; LF, low frequency; M, male; MD, memory deterioration; NA, not available; OD, right eye; od, olfactory decline; OS, left eye; R, red; RAPD, relative afferent pupillary defect; T, total; TOF, tetralogy of Fallot; Y, yellow. —, absent; #, new symptoms occurred during telephone follow-up.

mechanisms of the two CNVs (Supplementary Tables S5 and S6). For the 70 kb deletion, a five-bp microhomology domain "gcagc" was identified at the breakpoint. For the 256 bp duplication, a three-bp microhomology domain "AGG" was confirmed at the breakpoint (Fig. 2). Several repeated sequences or non-B DNA forming motifs were found at the breakpoint (Supplementary Table S6). The large duplication in exon 8 was predicted to cause frameshift coding, which generated a PTC at codon 627.

Clinical Findings

In the current cohort, 23 probands (16 males and 7 females) carried biallelic disease-causing *WFS1* variants, which were confirmed by cosegregation analyses (Table 2). The patients' mean age at last examination was 17.2±10.6 (range 6–43) years. As the patients were evaluated at an ophthalmic research institution, OA was observed in all the patients, followed by DM in 21 patients (91.3%), D in nine patients (39.1%), UD in nine patients (39.1%), and DI in five patients (21.7%). The mean or median onset ages for each clinical feature are summarized in Table 3. The four clinical manifestations of DIDMOAD occurred in the following order, from first to last: DM, D, OA, and DI. The mean onset age for DM, OA, and D was younger than 15 years. Only two patients (A1972 and A3790) had developed all four components at their last examination. Three patients (A600, A2018, and A3989) experienced four clinical features (OA, DM, UD, and either D or DI) and 11 probands suffered with three clinical signs (OA, DM, and either D, DI, or UD), whereas the remaining seven patients presented only OA with DM (six patients) or UD (one patient). The main clinical

Table 3. Demographics and Systemic Characteristics of Patients With WFS1

			Age (Year)		
Clinical Manifestations	Patient Number	Percentage	Mean ± SD	Media	Range
Major clinical manifestations					
DM	21	91.3%	9.6 ± 8.0	8.0	2–32
OA	23	100.0%	12.4 ± 7.4	9.0	4–33
D	9	39.1%	10.0 ± 2.8	10.0	5–15
DI	5	21.7%	16.6 ± 14.1	13.0	5–41
Other system manifestations					
Urinary tract dysfunction	9	39.1%	18.7 ± 12.9	16.0	6–41
Balance impairment	3	13.0%	6.7 ± 0.6	7.0	6–7
Olfactory decline	2	8.7%	/	33.0	24, 42
Psychiatric symptoms	2	8.7%	/	11.5	7, 16
Died	1	4.3%	/	13.0	/
Fecal incontinence	1	4.3%	/	16.0	/
Memory deterioration	1	4.3%	/	14.0	/
Tetralogy of Fallot	1	4.3%	/	0.5	/

SD, standard deviation.

Investigative Ophthalmology & Visual Science

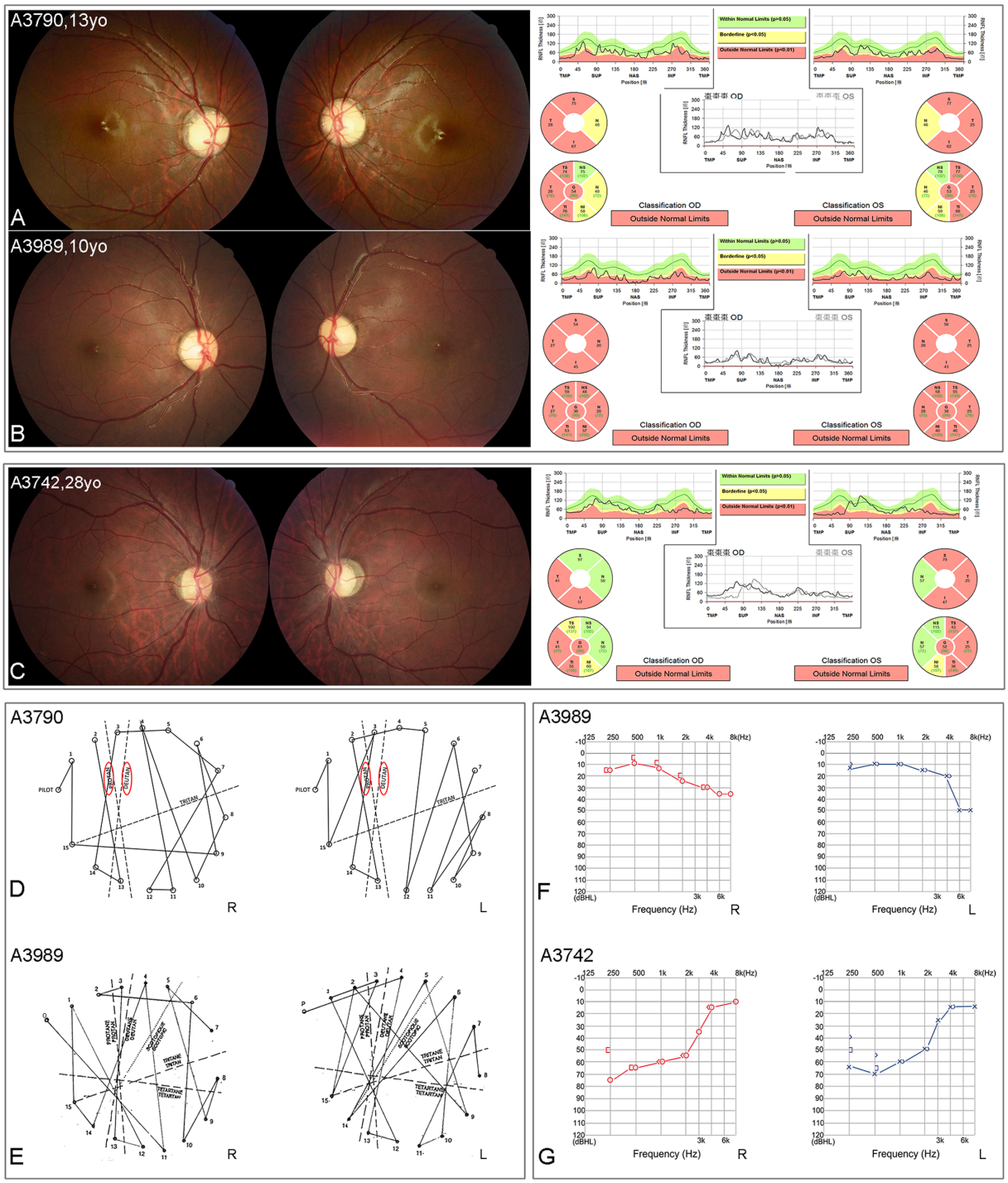

Figure 3. Colored fundus (CF) photographs, OCT scanning of the optic disc, color perception test (CPT), and pure tone audiometry (PTA) results of three patients in the current study. (**A, B**) CF photographs and OCT images of patients A3790 and A3989 harboring biallelic variants of *WFS1*, show nearly total and total optic disc pallor and retinal nerve fiber layer (RNFL) thinning in the temple or total quadrants. (**C**) Optic disc appearance and OCT examination of patient A3742 carrying monoallelic variant display temporal pallor and the RNFL thinning. (**D, E**) CPTs of patients A3790 and A3989 exhibit red/green color vision defect and total color blindness. (**F**) PTA of patient A3989 displays high-frequency hearing impairments. (**G**) PTA of patient A3742 presents low-frequency hearing impairments.

characteristics of each patient are summarized in Table 2. Some patients also experienced olfactory decline, balance impairment, memory deterioration, and tetralogy of Fallot (Table 3). One patient (A3537) died at age 13 years, according to our telephone survey.

Ophthalmic Features

All the patients had different extent visual defects, and their mean BCVA (logMAR) was 0.79 ± 0.49 (range 0.1–1.85). One patient presented with mild nystagmus. Lens opacity

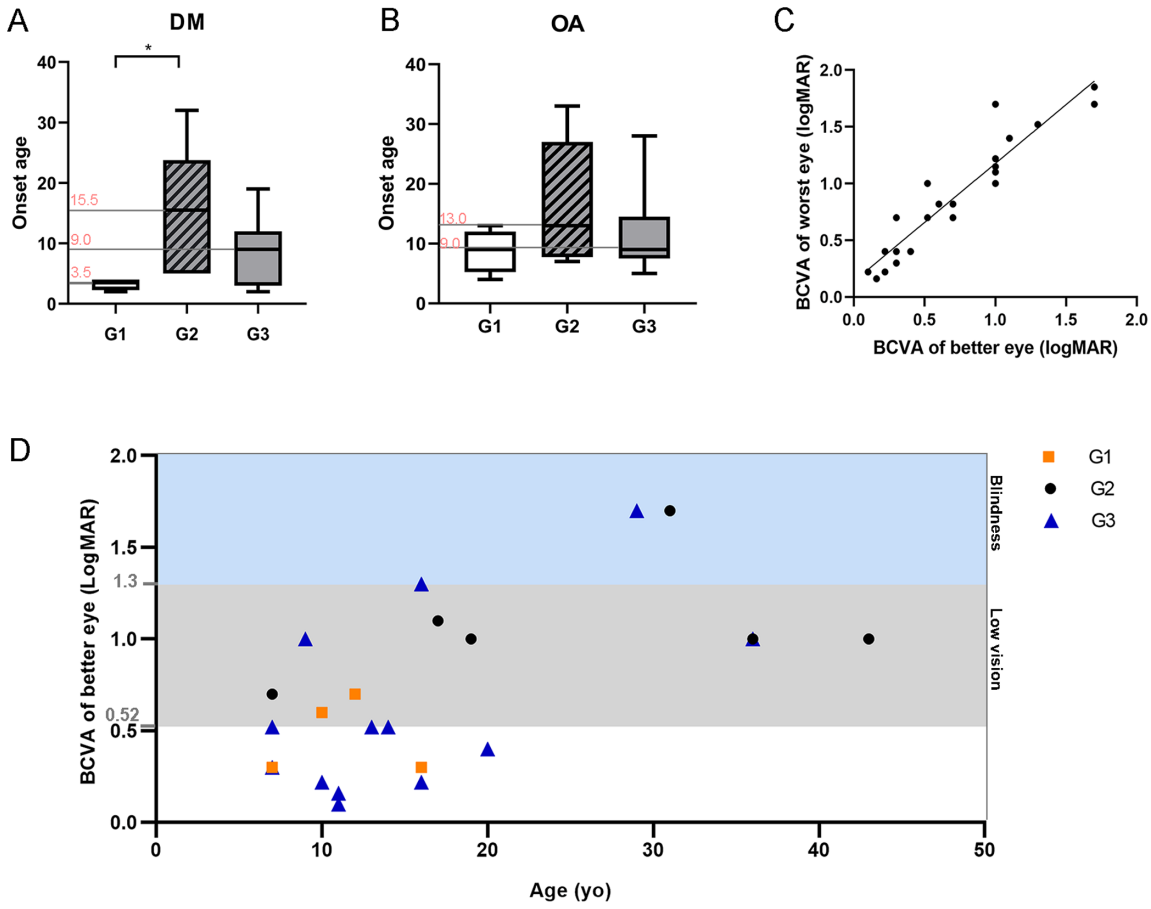

Figure 4. Comparison of the mean onset age for DM and OA between the patients with different genotypes and BCVA as a function of age in the 23 patients with genetic confirmed WFS1. (**A, B**) Comparison of the mean onset age for DM and OA in the patients in different groups (G). G1, patients carrying biallelic null variants; G2, patients harboring a biallelic missense variant; G3, patients carrying one missense variant combined with one null variant. *$P = 0.014$. (**C**) Symmetry between the BCVA of the better- and worse-seeing eyes of the 23 patients. A strong correlation coefficient was found ($r = 0.9407$; $P < 0.0001$). (**D**) Scatterplot for the BCVA as a function of age in the better seeing eyes of the patients in the different groups, indicated by *orange rectangles*, *black dots*, and *blue triangles*.

was observed in six patients. Fundus examination revealed a symmetrical total (60.9%) or whole temporal disc pallor in all the patients (Figs. 3A, 3B). Overall, 18 patients (36 eyes) underwent retinal OCT scans, and 15 of those patients presented symmetrical OCT findings. Of the 36 eyes, 20 eyes (55.6%) showed total diffuse retinal nerve fiber layer (RNFL) defects or thinning in all six quadrants: temporal (T), temporal superior (TS), temporal inferior (TI), nasal (N), nasal superior (NS), and nasal inferior (NI). The remaining 18 eyes displayed substantial RNFL thinning in the TS, T, and TI quadrants, while the RNFL in the NS, N, and NI remained relatively normal or subnormal (Figs. 3A, 3B). Of the 17 patients (34 eyes) who underwent a color perception test, 21 eyes exhibited a red/green color vision defect (Fig. 3D), 11 eyes showed total color blindness (Fig. 3E), and two eyes had yellow/blue color vision deficiency.

Genotype–Phenotype Correlation

We divided the 23 patients with genomic confirmed WFS1 into three groups based on their genotypes. Patients in Group 1 carried biallelic null variants, which included nonsense, frame-shift variants, splicing effect, multiple amino acid insertion/deletions, and CNVs. Patients in Group 2 harbored biallelic missense or single amino acid insertion/deletion variations. Patients in Group 3 carried missense or single amino acid insertion/deletion variants combined with a null variant. We found that the mean onset ages for DM and OA were younger in the patients in Group 1 than in Group 2; however, only the difference for DM reached statistical significance ($P = 0.014$) (Figs. 4A, 4B).

All patients presented with severe visual defects; over half of them met the standard of low vision according to WHO criteria when they were under 20 years, and all patients reached the standard of low vision or blind when they were older than 20 years (Figs. 4C, 4D). The extent of visual impairment was not related to the patient genotype (Fig. 4D).

In the current cohort, patient A3742 was the only patient who had one heterozygous missense variant p. (Arg859Pro). That patient was a 28-year-old male, and his fundus examination revealed bilateral temporal optic pallor and RNFL thinning in the TS and TI quadrants (Fig. 3C). Cosegregation analysis revealed that the patient's mother also harbored the same variant. He and his mother both had a low-frequency hearing loss (Fig. 3G), which was different from the high-frequency hearing defects usually observed in patients with biallelic variants (Fig. 3F).

Investigative Ophthalmology & Visual Science

Discussion

In this study, we performed comprehensive genetic analyses and determined the clinical findings in a Chinese cohort with WFS1 from a tertiary center. We observed that four of the 24 patients (16.7%) had only one heterozygous variant detectable by Sanger DNA sequencing of the coding regions in *WFS1*, but this rate was much higher than previously reported (4.5%–8.3%).[2,11] Our WGS analysis identified the missing heritability in three of the four patients (75%) as one DIV, one large duplication, and one point variant in the 5′UTR splice site. Our results further indicated the significance of screening the noncoding region or CNVs when conducting genetic analysis of *WFS1*.

The 38 distinct pathogenic variants detected in the current study encompassed all types of pathogenic variants in *WFS1*. Consistent with previous studies,[2–4,6,11] almost 90% of the variants identified in the current cohort were clustered in exon 8. CNVs were very rare in the *WFS1* gene, and only three large deletions have been reported previously.[12–14] In the current cohort, we identified two novel CNVs, with a 70 kb deletion that is, so far, the largest deletion detected and covered the entire *WFS1* gene and its associated regulatory region. Similarly, the large duplication reported here is the first large duplication (>100 bp) detected in the *WFS1* gene. We also validated the breakpoints of the two CNVs, and we identified two microhomology domains at the breakpoints by combining whole genome sequencing data analysis and Sanger sequencing. The microhomology at the breakpoints suggested that the CNVs belonged to nonrecurrent rearrangements and that the underlying mechanisms might involve nonhomologous end joining or microhomology-mediated end joining.[19]

Our in vitro functional analysis results indicated that the DIV c.712+681C>T activated cryptic splice donor sites to produce two abnormal splicing products containing insertions of PEs. The PE insertions altered the reading frame and led to a PTC. Our minigene analysis revealed that the DIV generated both normal and abnormal splicing products. This was consistent with previous observations in other inherited retinal dystrophy genes, such as *ABCA4*.[20] For example, Sangermano et al.[20] also observed both correct and mutant transcripts in the majority of the DIVs detected in *ABCA4,* but the fraction of mutant transcripts differed (from 8% to 93%) for each DIV. We did not perform quantitative analysis of the RT-PCR products, so we were unable to determine or predict the mutant pathogenic strengths caused by the DIV c.712+681C>T.

The novel variant c.−6+6T>C was another missing variant revealed by whole genome sequencing. This variant, located in intron 1, was a splicing variant in the noncoding region (5′ UTR) of *WFS1* and was predicted by the NetUTR server to eliminate the original first splice-donor site. Splice site recognition in 5′ UTRs remains challenging; therefore bioinformatics analysis for this kind of variant is very rare.[21,22] This novel variant was not recorded in any public database, the base "T" was highly conserved among mammals, such as mouse, elephant, macaque, and gorilla, and the variant cosegregated in patient A3537's pedigree. Therefore we defined it as likely pathogenic, based on the ACMG standard. Unfortunately, we could not obtain blood samples for RNA analysis from this patient and his parents. We plan to conduct in vitro expression analysis in the future to verify the impact of this variant on *WFS1* expression.

The patients in the current cohort exhibited high variations in their phenotypes. The proportion of patients presenting the four clinical components of DIDMOAD was only 8.7% (2/23), which was a much lower value than previously described (46.7%–53%).[2,5,6] We speculate that this lower proportion might reflect the small number of patients who carry biallelic null variants. DM and OA are two critical clinical features of WFS1 and usually appear before 15 years of age. We observed three patients (A534, A600, and A610) who developed DM after 20 years, and all of them carried homozygous or compound heterozygous missense variants. Chaussenot et al.[13] also reported that late-onset WFS1 is usually associated with missense variations. Our genotype-phenotype analysis further revealed that the onset age of DM was significantly earlier in patients with biallelic null variants than with biallelic missense variants. These findings were similar with the results reported previously in several studies.[2,5,14] Previous research has indicated that patients with a whole exon 8 deletion or complex structural rearrangement develop a severe WFS1 phenotype that results in early death, or they show a complex phenotype with a neonatal-onset DI, optic pathway hypoplasia, and psychomotor retardation.[12,14] Patient A3784, who carried the homozygous novel 70 kb deletion, only had DM, OA, and D at 12 years of age, and her brain magnetic resonance imaging scan did not show any central nervous system abnormalities. She had an early-onset age (three years) of DM, followed by nine years for the onset of OA and D. She suffered memory deterioration at 14 years of age, according to our telephone follow-up. Patient A3742, who carried the heterozygous missense variant, displayed typical clinical features of WFSL, and the missense variant was located in the C-terminal of the WFS1, in agreement with previous observations.[15,23]

Detailed ophthalmologic characteristics have been lacking for patients with genetically confirmed WFS1. Our patients had severe visual defects, and their mean BCVA (logMAR) was worse than the value of 0.33 reported in 18 American patients,[24] but it was better than the 1.10 described in 13 Turkish patients.[25] We speculate that these differences might reflect the different mean ages of the patients in the different studies, because our results indicated a decrease in BCVA with patient aging. We did not observed a relationship between the extent of the visual defect and the patient genotype, but this might be due to the small number of patients in each group. Fundus examination showed total optic disc pallor in more than 60% of the patients, whereas a prominent temporal wedge of pallor was not seen in any patients. These findings differed from the optic disc appearance reported for patients with autosomal dominant optic atrophy, which is mainly caused by pathogenic variants of *OPA1*.[26,27] A prominent temporal wedge of pallor is a main fundus feature of patients carrying *OPA1* variants, which are usually observed in 60% to 86% of the eyes.[26,27]

In accordance with the fundus findings, the retinal OCT scanning revealed diffuse and substantial RNFL thinning in all the eyes, with more than 60% of them showing involvement of whole quadrants and less than 40% of the eyes having almost normal or less thinning in the nasal quadrant. A previous study that included 18 American patients reported that the topography of RNFL thinning from severe to mild was superior, inferior, temporal, and nasal quadrant.[24] Consistent with the observations from two previous studies,[24,25] our patients all suffered from dyschromatopsia, and most of these were red-green perception deficits.

The current study has some limitations, including its retrospective design and the incomplete physical examinations for other tissues or organs except the eye. We also

did not perform any quantitative assessment for retinal OCT; therefore we cannot precisely define the extent of the RNFL thinning in our patients.

In conclusion, our results extend the pathogenic variant spectrum of *WFS1*. WGS revealed the missing heritability of the patients who had only a monoallelic variant identified. The DIVs and CNVs explained the rare unresolved Chinese cases of WFS1. Patients with WFS1 might show wide and variable clinical spectra; therefore genetic analysis is vital for the precise diagnosis of patients with atypical WFS1.

Acknowledgments

Supported by the National Key R&D Program of China, 2016YFC0905200. The funding organization had no role in designing or conducting this research.

Disclosure: **X. Zhang,** None; **Y. Xie,** None; **K. Xu,** None; **H. Chang,** None; **X. Zhang,** None; **Y. Li,** None

References

1. Moosajee M, Yu-Wai-Man P, Rouzier C, Bitner-Glindzicz M, Bowman R. Clinical utility gene card for: Wolfram syndrome. *Eur J Hum Genet.* 2016;11:1–4.
2. Rigoli L, Aloi C, Salina A, et al. Wolfram syndrome 1 in the Italian population: genotype-phenotype correlations. *Pediatr Res.* 2020;87:456–462.
3. Lombardo F, Salzano G, Di Bella C, et al. Phenotypical and genotypical expression of Wolfram syndrome in 12 patients from a Sicilian district where this syndrome might not be so infrequent as generally expected. *J Endocrinol Invest.* 2014;37:195–202.
4. Ganie MA, Laway BA, Nisar S, et al. Presentation and clinical course of Wolfram (DIDMOAD) syndrome from North India. *Diabet Med.* 2011;28:1337–1342.
5. Barrett TG, Bundey SE, Macleod AF. Neurodegeneration and diabetes: UK nationwide study of Wolfram (DIDMOAD) syndrome. *Lancet.* 1995;346:1458–1463.
6. Matsunaga K, Tanabe K, Inoue H, et al. Wolfram syndrome in the Japanese population; molecular analysis of WFS1 gene and characterization of clinical features. *PLoS One.* 2014;9:e106906.
7. Tranebjærg L, Barrett T, Rendtorff ND. WFS1 Wolfram syndrome spectrum disorder. In: Adam MP, Ardinger HH, Pagon RA, et al. eds. *GeneReviews.* Seattle: University of Washington; 1993.
8. Inoue H, Tanizawa Y, Wasson J, et al. A gene encoding a transmembrane protein is mutated in patients with diabetes mellitus and optic atrophy (Wolfram syndrome). *Nat Genet.* 1998;20:143–148.
9. Takeda K, Inoue H, Tanizawa Y, et al. WFS1 (Wolfram syndrome 1) gene product: predominant subcellular localization to endoplasmic reticulum in cultured cells and neuronal expression in rat brain. *Hum Mol Genet.* 2001;10:477–484.
10. Hofmann S, Philbrook C, Gerbitz KD, Bauer MF. Wolfram syndrome: structural and functional analyses of mutant and wild-type wolframin, the WFS1 gene product. *Hum Mol Genet.* 2003;12:2003–2012.
11. de Heredia ML, Clèries R, Nunes V. Genotypic classification of patients with Wolfram syndrome: insights into the natural history of the disease and correlation with phenotype. *Genet Med.* 2013;15:497–506.
12. Smith CJ, Crock PA, King BR, Meldrum CJ, Scott RJ. Phenotype-genotype correlations in a series of wolfram syndrome families. *Diabetes Care.* 2004;27:2003–2009.
13. Chaussenot A, Rouzier C, Quere M, et al. Mutation update and uncommon phenotypes in a French cohort of 96 patients with WFS1-related disorders. *Clin Genet.* 2015;87:430–439.
14. Elli FM, Ghirardello S, Giavoli C, et al. A new structural rearrangement associated to Wolfram syndrome in a child with a partial phenotype. *Gene.* 2012;509:168–172.
15. Kobayashi M, Miyagawa M, Nishio SY, et al. WFS1 mutation screening in a large series of Japanese hearing loss patients: Massively parallel DNA sequencing-based analysis. *PLoS One.* 2018;13:e0193359.
16. Rendtorff ND, Lodahl M, Boulahbel H, et al. Identification of p.A684V missense mutation in the WFS1 gene as a frequent cause of autosomal dominant optic atrophy and hearing impairment. *Am J Med Genet. A* 2011;155a:1298–1313.
17. Jeon SA, Park JL, Park SJ, et al. Comparison between MGI and Illumina sequencing platforms for whole genome sequencing. *Genes Genomics.* 2021;43:713–724.
18. Rao J, Peng L, Liang X, et al. Performance of copy number variants detection based on whole-genome sequencing by DNBSEQ platforms. *BMC Bioinformatics.* 2020;21:518.
19. Carvalho CM, Lupski JR. Mechanisms underlying structural variant formation in genomic disorders. *Nat Rev Genet.* 2016;17:224–238.
20. Sangermano R, Garanto A, Khan M, et al. Deep-intronic ABCA4 variants explain missing heritability in Stargardt disease and allow correction of splice defects by antisense oligonucleotides. *Genet Med.* 2019;21:1751–1760.
21. Eden E, Brunak S. Analysis and recognition of 5' UTR intron splice sites in human pre-mRNA. *Nucleic Acids Res.* 2004;32:1131–1142.
22. Davuluri RV, Grosse I, Zhang MQ. Computational identification of promoters and first exons in the human genome. *Nat Genet* 2001;29:412–417.
23. Grenier J, Meunier I, Daien V, et al. WFS1 in optic neuropathies: mutation findings in nonsyndromic optic atrophy and assessment of clinical severity. *Ophthalmology* 2016;123:1989–1998.
24. Hoekel J, Chisholm SA, Al-Lozi A, Hershey T, Tychsen L. Ophthalmologic correlates of disease severity in children and adolescents with Wolfram syndrome. *J AAPOS* 2014;18:461–465.e461.
25. Ustaoglu M, Onder F, Karapapak M, Taslidere H, Guven D. Ophthalmic, systemic, and genetic characteristics of patients with Wolfram syndrome. *Eur J Ophthalmol.* 2020;30:1099–1105.
26. Yu-Wai-Man P, Griffiths PG, Burke A, et al. The prevalence and natural history of dominant optic atrophy due to OPA1 mutations. *Ophthalmology.* 2010;117:1538–1546,e1531.
27. Chen J, Xu K, Zhang X, et al. Mutation screening of mitochondrial DNA as well as OPA1 and OPA3 in a Chinese cohort with suspected hereditary optic atrophy. *Invest Ophthalmol Vis Sci.* 2014;55:6987–6995.
28. Cano A, Rouzier C, Monnot S, et al. Identification of novel mutations in WFS1 and genotype-phenotype correlation in Wolfram syndrome. *Am J Med Genet A.* 2007;143a:1605–1612.
29. Nakamura A, Shimizu C, Nagai S, et al. A novel mutation of WFS1 gene in a Japanese man of Wolfram syndrome with positive diabetes-related antibodies. *Diabetes Res Clin Pract.* 2006;73:215–217.
30. Zmyslowska A, Borowiec M, Antosik K, et al. Wolfram syndrome in the Polish population: novel mutations and genotype-phenotype correlation. *Clin Endocrinol (Oxf).* 2011;75:636–641.
31. Hong J, Zhang YW, Zhang HJ, et al. The novel compound heterozygous mutations, V434del and W666X, in WFS1

gene causing the Wolfram syndrome in a Chinese family. *Endocrine*. 2009;35:151–157.

32. Strom TM, Hörtnagel K, Hofmann S, et al. Diabetes insipidus, diabetes mellitus, optic atrophy and deafness (DIDMOAD) caused by mutations in a novel gene (wolframin) coding for a predicted transmembrane protein. *Hum Mol Genet*. 1998;7:2021–2028.
33. Astuti D, Sabir A, Fulton P, et al. Monogenic diabetes syndromes: Locus-specific databases for Alström, Wolfram, and Thiamine-responsive megaloblastic anemia. *Hum Mutat*. 2017;38:764–777.
34. Gasparin MR, Crispim F, Paula SL, et al. Identification of novel mutations of the WFS1 gene in Brazilian patients with Wolfram syndrome. *Eur J Endocrinol*. 2009;160:309–316.

Investigative Ophthalmology & Visual Science